

Magnetic Fields in Galaxy Clusters

Federica Govoni

Dip. Astronomia, Univ. Bologna, Via Ranzani 1, Bologna, Italy

Matteo Murgia

Ist. di Radioastronomia del CNR, Via Gobetti 101, Bologna, Italy

Abstract. Magnetic fields in galaxy clusters can be investigated using a variety of techniques. Recent studies including radio halos, Inverse Compton hard X-ray emissions and Faraday rotation measure, are briefly outlined. A numerical approach for investigating cluster magnetic fields strength and structure is presented. It consists of producing simulated rotation measure, radio halo images, and radio halo polarization, obtained from 3-dimensional multi-scale cluster magnetic field models, and comparing with observations.

1. Magnetic Field Measures

A complete description of the astrophysical processes in cluster of galaxies requires knowledge of magnetic fields. The most detailed evidence for this component comes from the radio observations:

- Some clusters of galaxies exhibit diffuse non-thermal synchrotron radio halos, associated with the intra-cluster medium, which extend up to Mega-parsec scales. Using minimum energy assumptions, it is possible to estimate an equipartition magnetic field strength averaged over the entire halo volume. These estimates give equipartition magnetic field strengths of $\simeq 0.1$ to $1 \mu\text{G}$ (e.g. Bacchi et al. 2003).
- In a few cases, clusters containing a radio halo show an excess emission. This emission could be interpreted in terms of Inverse Compton scattering of the cosmic microwave background photons with the relativistic electrons responsible for the radio halo emission. In this case, the measurements of the magnetic field strength (e.g. Fusco-Femiano et al. 1999, Rephaeli et al. 1999) inferred from the ratio of the radio to X-ray luminosities are consistent with the equipartition estimates.
- Indirect measurements of the magnetic field intensity can also be determined in conjunction with X-ray observations of the hot gas, through the study of the Faraday Rotation Measure (RM) of radio sources located inside or behind clusters. By using a simple analytical approach, magnetic fields of $\sim 5 - 30 \mu\text{G}$, have been found in cooling flow clusters (e.g. Allen et al. 2001; Taylor & Perley 1993) where extremely high RMs have been revealed. On the other hand, significant magnetic fields have also been detected in clusters without cooling flows: the RM measurements of polarized radio sources through the hot intra-cluster medium leads to a magnetic field of $2 - 8 \mu\text{G}$ which fluctuates on scales as small

as 2 – 15 kpc. (e.g. Feretti et al. 1995, Feretti et al. 1999, Clarke et al. 2001, Govoni et al. 2001, Taylor et al. 2001, Eilek & Owen 2002).

The magnetic field strength obtained by RM studies is therefore higher than the value derived from the radio halo data and from Inverse-Compton X-ray studies. However, as pointed out by Carilli & Taylor (2002) and references therein, all the aforementioned techniques are based on several assumptions. For example, the observed RMs have been interpreted, until now, in terms of simple analytical models which consider single-scale magnetic fields. On the other hand, magneto-hydrodynamic cosmological simulations (Dolag et al. 2002) suggest that cluster magnetic fields may span a wide range of spatial scales with a strength that decreases with distance from the cluster center.

We developed a numerical approach for investigating the strength and structure of cluster magnetic fields. It consists of comparing simulated rotation measure, radio halo images, and radio halo polarization, obtained from 3-dimensional multi-scale cluster magnetic field models, with observations (Murgia et al. 2003, submitted).

2. Simulated Rotation Measures

The RM is related to the thermal electron density, n_e , and magnetic field along the line-of-sight, B_{\parallel} , through the cluster by the equation:

$$\text{RM} = 812 \int_0^L n_e B_{\parallel} dl \quad \text{rad m}^{-2} \quad (1)$$

where B_{\parallel} is measured in μG , n_e in cm^{-3} and L is the depth of the screen in kpc.

We consider a multi-scale magnetic field model with a three-dimensional power spectrum: $|B_k|^2 \propto k^{-n}$. Different power spectrum index will generate different magnetic field configurations and therefore will give rise to very different simulated RM images.

Fig. 1 (top) shows simulated RM images with different values of the index n for a typical cluster of galaxies (see caption for more details). RM images, such as those we simulate, cannot be observed for real clusters of galaxies. However, it is relatively easy to measure the RM dispersion and mean (σ_{RM} and $\langle \text{RM} \rangle$) in limited regions by observing radio sources located at different projected distances from the cluster center. Fig. 1 (bottom) shows the simulated profiles of σ_{RM} (left), $|\langle \text{RM} \rangle|$ (center), and $|\langle \text{RM} \rangle|/\sigma_{\text{RM}}$ (right), as a function of the distance from the cluster center. While both σ_{RM} and $|\langle \text{RM} \rangle|$ increase linearly with the cluster magnetic field strength, the ratio $|\langle \text{RM} \rangle|/\sigma_{\text{RM}}$ depends only on the magnetic field power spectrum slope for a given range of fluctuation scales. This means that the comparison of RM data of radiogalaxies embedded in a cluster of galaxies with simulated profiles, can infer the strength and the power spectrum slope of the cluster magnetic field. The comparison of our simulations with data (Murgia et al. 2003, submitted), indicates magnetic field strengths a factor of ~ 2 lower than that predicted by the single-scale magnetic field approximation widely used in the literature, and a rather flat spectral index $n \simeq 2$.

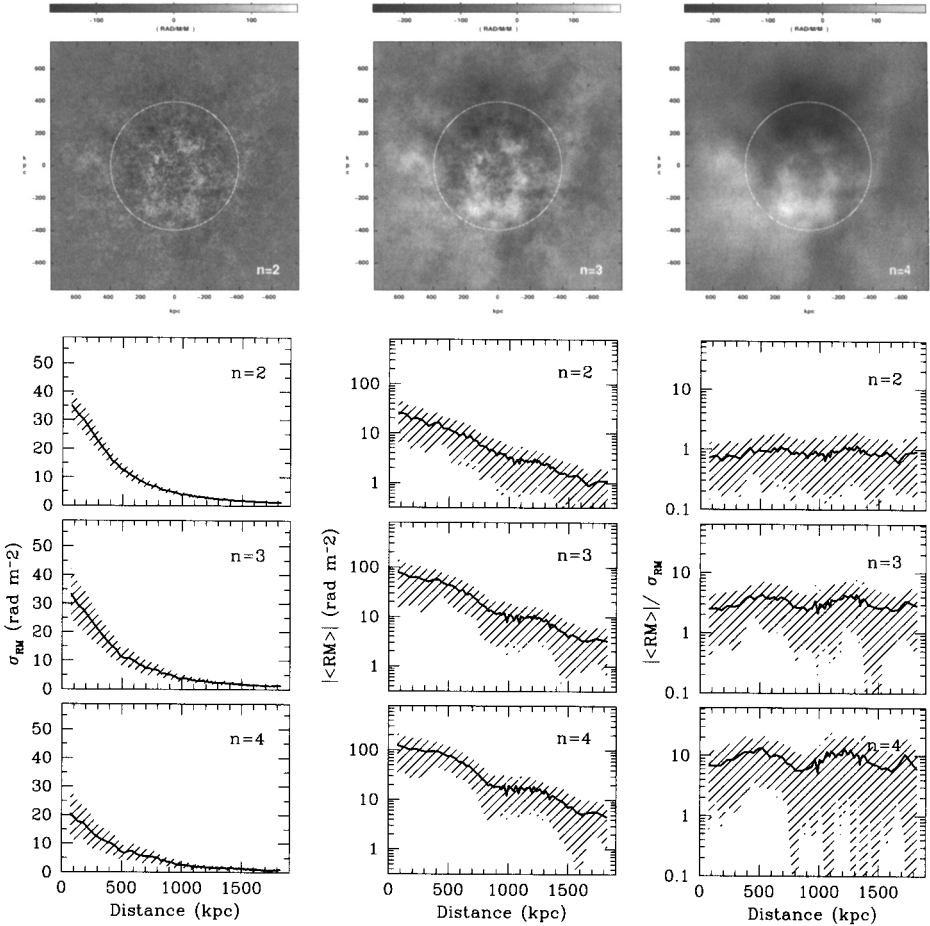


Figure 1. **Top:** simulated RM images for magnetic field power spectrum spectral index $n = 2, 3, 4$. The electron gas density of the cluster follow a standard β -model with a core radius $r_c=400$ kpc (indicated by a circle in the figure) a central density $n_e(0)=10^{-3} \text{ cm}^{-3}$ and $\beta=0.6$. The three power spectra are normalized to have the same total magnetic field energy which is distributed over the range of spatial scales from 6 kpc up to 770 kpc. The field at the cluster center is $\langle \mathbf{B} \rangle_0 = 1 \mu\text{G}$ and its energy density decreases from the cluster center according to $B^2 \propto n_e(r)$. **Bottom:** radial profiles (σ_{RM} , $|\langle \text{RM} \rangle|$ and $|\langle \text{RM} \rangle|/\sigma_{\text{RM}}$ respectively) obtained from the RM simulations described above. The profiles have been obtained by averaging the simulated RM images in regions of $50 \times 50 \text{ kpc}^2$, which is a typical size for radio galaxies.

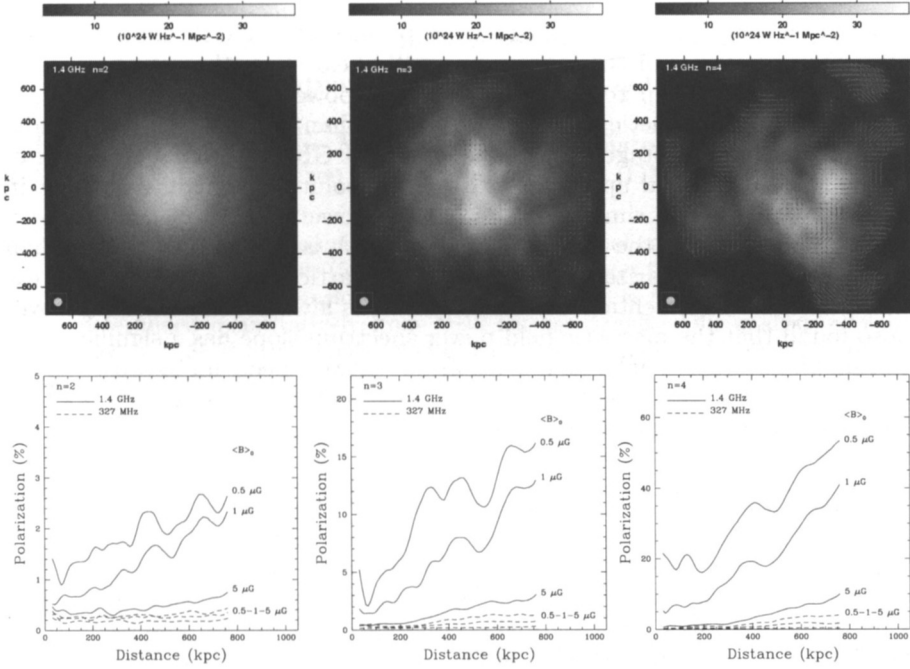


Figure 2. Simulated halo brightness and polarization for cluster at a distance of $z = 0.05$ as it would be observed with a beam of $45''$ ($H_0 = 50 \text{ km s}^{-1} \text{ Mpc}^{-1}$). **Top**: simulated halo images at 1.4 GHz for different values of the magnetic field power spectrum slope n and $\langle B \rangle_0 = 1 \mu\text{G}$; the vectors lengths are proportional to the degree of polarization, with 100 percent corresponding to 100 kpc on the sky. Field directions are those of the E-vector. **Bottom**: radially averaged profiles of the polarization percentage at 327 MHz and 1.4 GHz for three values of the magnetic field strength, namely $\langle B \rangle_0 = 0.5, 1$ and $5 \mu\text{G}$.

3. Simulated Radio Halo Images and Radio Halo Polarization

Radio halo observations may provides important information about the cluster magnetic field structure since different values of the power spectrum spectral index will generate very different total intensity and polarization brightness distributions for the radio halo emission.

So far, polarization emission from radio halos has not been detected. The current upper limits to the polarization at 1.4 GHz, for beams of about $45''$, are a few percent (3 – 4%).

We simulated the expected total intensity and polarization brightness distribution at 1.4 GHz and 327 MHz, as it would be observed with a beam of $45''$, for different values of the magnetic field strength and power spectrum index, by introducing in the 3-dimensional magnetic field an isotropic population of relativistic electrons.

Fig. 2 (top) shows simulated radio halo brightness and polarization percentage distributions at 1.4 GHz (see caption for more details). Fig. 2 (bottom)

shows the expected fractional polarization profiles at 1.4 GHz and 327 MHz for the different values of the average magnetic field strength and power spectrum spectral index. Our results indicate that a power spectrum slope steeper than $n = 3$ and a magnetic field strength lower than $\sim 1 \mu\text{G}$ result in a radio halo polarization percentage at a frequency of 1.4 GHz that is far in excess of the current observational upper limits at $45''$ resolution. This means that, in agreement with the RM simulations, either the power spectrum spectral index is flatter than $n = 3$ or the magnetic field strength is significantly higher than $\sim 1 \mu\text{G}$. The halo depolarization at 327 MHz is particularly severe and the expected polarization percentage at this frequency is always below 1%. Moreover we also found that the magnetic field power spectrum slope has a significant effect in shaping the radio halo. In particular, flat power spectrum indexes ($n < 3$) give rise to very smooth radio brightness images (under the assumption that the radiating electrons are uniformly distributed).

4. Conclusions

The numerical approach presented here demonstrates how the dispersion and mean of the RM measured in radio galaxies embedded in a cluster of galaxies can be used to constrain not only the strength but also the power spectrum slope of the intra-cluster magnetic fields. Moreover, the study of the polarization properties of a large scale radio halo, if it is present in a cluster, can be used to improve the estimates based on the RM analysis.

Acknowledgment. We thank L. Feretti, G. Giovannini, D. Dallacasa, R. Fanti, G.B. Taylor and K. Dolag for their collaboration.

References

- Allen S.W., Taylor G.B., Nulsen P.E.J., et al., 2001, MNRAS 324, 842
Bacchi M., Feretti L., Giovannini G., & Govoni F., 2003, A&A 400, 465
Carilli C.L., Taylor G.B., 2002, ARA&A, 40, 319
Clarke T.E., Kronberg P.P., Böhringer H., 2001, ApJ 547, L111
Dolag K., Bartelmann M., Lesch H., 2002, A&A 387, 383
Eilek J.A., Owen F.N., 2002, ApJ, 567, 2002
Feretti L., Dallacasa D., Giovannini G., Tagliani A., 1995, A&A 302, 680
Feretti L., Dallacasa D., Govoni F., et al., 1999, A&A 344, 472
Fusco-Femiano R., dal Fiume D., Feretti L., et al., 1999, ApJ 513, L21
Govoni F., Taylor G.B., Dallacasa D., et al., 2001, A&A 379, 807
Murgia, M., Govoni, F., Feretti, L., Giovannini, G., Dallacasa, D., Fanti, R., Taylor, G. B., Dolag K. 2004 A&A, 424, 429
Rephaeli Y., Gruber D., Blanco P., 1999, ApJ 511, L21
Taylor G.B., Perley R.A., 1993, ApJ, 416, 554
Taylor G.B., Govoni F., Allen S., Fabian A.C., 2001, MNRAS 326, 2